Applied Catalysis B: Environmental 343 (2024) 123528

Contents lists available at ScienceDirect

Applied Catalysis B: Environmental

journal homepage: www.elsevier.com/locate/apcatb

CO_2-assisted propane dehydrogenation to aromatics over copper modified Ga-MFI catalysts

Kankan Bu, Yikun Kang, Yefei Li *, Yahong Zhang, Yi Tang, Zhen Huang *, Wei Shen, Hualong Xu *

Department of Chemistry, Shanghai Key Laboratory of Molecular Catalysis and Innovative Materials and Laboratory of Advanced Materials, Collaborative Innovation Center of Chemistry for Energy Materials, Fudan University, Shanghai 200433, PR China

ARTICLE INFO

Keywords:
CO_2-assisted propane aromatization
Ga-MFI zeolite
Cu modification
Brønsted/Lewis acid ratio
Aromatics selectivity

ABSTRACT

The acidity and Ga-species status in the zeolite play a crucial role in the CO_2-assisted propane dehydroaromatization (CO_2-PDA). In this work, a copper modified Ga-MFI zeolite (Cu/Ga-MFI) with well dispersed framework Ga species was fabricated. A remarkable aromatics selectivity of 73% at propane conversion of 93.6% was achieved on Cu/Ga-MFI catalyst. The Ga atoms in MFI framework can create a moderate acid strength, while the introduced Cu provide an appropriate Brønsted/Lewis acid distribution, enhancing the synergy between metal-related species and the zeolite. Besides, DFT results indicate that the acid sites in Ga-MFI are more preferable for the dehydrogenation of propane instead of the C-C cleavage. Moreover, CO_2 can inhibit coke formation through reverse Boudouard and reverse water gas shift reaction, which endows Cu/Ga-MFI catalyst with superior anti-coking ability and regeneration stability. This work provides a novel approach for designing catalysts with high activity, aromatics selectivity, and stability for CO_2-PDA reactions.

1. Introduction

Aromatics, especially the light aromatics (benzene, toluene, ethylbenzene and xylenes, BTEX), as one of the most important basic chemicals, are widely applied for the production of polymers, resins, and a large range of fine chemicals. Conventionally, aromatics are produced from petroleum cracking, which has become more and more scarce with the growing shortage of petroleum resources. Therefore, it is urgent to develop non-petroleum feedstock for production of aromatics [1,2]. UOP (Universal Oil Products) and BP (British Petroleum) jointly developed a Cyclar process for the aromatization of light alkanes (mainly propane and butane) by using zeolite catalysts modified with gallium in early 1990 s. And this study sparked intensive research on the reaction schemes and mechanisms involved in this process in the next decade [3]. In recent years, with the increase in the supply of shale gas and related liquefied petroleum gas, research on the direct conversion of light alkanes into high-value added products has sprung up again. In this context, the direct conversion of propane to aromatics has become an important research topic, to which much effort has been dedicated [4,5]. A consensus mechanism for propane aromatization is that propane is first dehydrogenated into olefins, which are then oligomerized and cyclized into aromatics [6]. Since propane dehydrogenation reaction is an endothermic reaction and there is a balance restriction on the distribution of the products [7], which leads to low propane conversion rate, the catalyst is prone to coke deposition and deactivation. In order to overcome thermodynamic equilibrium limitations of this reaction, CO_2 is wildly adopted as a soft oxidant, which can consume produced H_2 and help coke oxidation, thus breaking the balance restriction and leading to an improved catalytic performance [8–12].

For propane aromatization, metal-modified zeolites are currently used as catalysts. The commonly used zeolites are MFI zeolites (mainly ZSM-5), while the active metals that are recognized to be more effective are Pt, Zn and Ga [2,13,14]. Due to the loss of the active component and poor selectivity for aromatics of Zn/ZSM-5, as well as the coke deposition and deactivation for both Zn/ZSM-5 and Pt/ZSM-5, a large amount of research has focused on Ga/ZSM-5 based catalysts. As described in the literature, the location, structure and chemical state of Ga species on ZSM-5 have a great impact on the performance of propane aromatization while it was closely related to the preparation method and treatment process of the catalyst [2]. The high dispersed Ga species exchange with Brønsted acid (B acid) protons will contribute to formation of strong Lewis acid (L acid) sites, and the synergistic effect between the B

* Corresponding authors.
E-mail addresses: yefeil@fudan.edu.cn (Y. Li), huangzhen@fudan.edu.cn (Z. Huang), shuhl@fudan.edu.cn (H. Xu).

https://doi.org/10.1016/j.apcatb.2023.123528
Received 23 August 2023; Received in revised form 12 November 2023; Accepted 13 November 2023
Available online 20 November 2023

acid and the Ga-related L acid can significantly improves propane conversion and aromatics selectivity [13]. For Ga/ZSM-5 prepared by wetness impregnation or ion exchange, due to the hydrated Ga^{3+} ion is too large to enter the micropores, the Ga species mainly distributed on the external surface of ZSM-5. Therefore, the activity, selectivity and stability of Ga/ZSM-5 in CO_2-PDA reaction are not satisfactory [15,16]. In order to improve the dispersion of Ga species, the research on preparation methods of Ga/ZSM-5 has been conducted extensively by researchers. Such as chemical vapor deposition [17], oxidation-reduction (H_2-O_2) pretreatment [15,18,19], acid post-treatment [13,20], etc.

Apart from the aforementioned methods, with direct addition of Ga precursor during zeolite preparation, one-step hydrothermal synthesis of galloaluminosilicate, and incorporation of Ga into the zeolite framework are also effective strategies to enhance Ga dispersion [2,6,21–24]. Al-Yassir et al. synthesized a gallium-aluminum-silicate zeolite (Ga-Al-Si zeolite) by directly introducing $Ga(NO_3)_3$ during the synthesis of ZSM-5 using a one-step hydrothermal method [25]. The synthesized Ga-Al-Si zeolite was then mixed with a solution of CTAB and NaOH for secondary crystallization, resulting in a Ga-Al-Si zeolite with an ordered mesoporous structure. This catalyst exhibited high propane conversion and aromatics selectivity in propane aromatization reaction. The improved catalytic performance is attributed to the in situ hydrothermal synthesis and the presence of ordered mesopores, which facilitate the infiltration of Ga atoms into the framework, leading to the formation of a higher concentration of framework Ga species. These framework Ga species are the actual active sites for alkane dehydroaromatization. Despite significant progress in enhancing the performance of Ga-based catalysts, several challenges persist. These include low yields of aromatics, rapid catalyst deactivation caused by coke deposition and regeneration issues. Thus, achieving high aromatics selectivity and high catalytic stability simultaneously is a long-term challenge for PDA reactions.

It is worth noting that incorporating Ga into the ZSM-5 framework has been demonstrated to improve the aromatics selectivity of the catalyst [26,27]. However, the presence of both Ga and Al in the zeolite framework often results in poor catalyst stability. This may be related to its strong acidity and high acid density leading to polycondensation of aromatic intermediates to form coke deposits [26]. Nevertheless, when the framework Al is isomorphous substituted by Ga, the strength of the acidity of bridged framework Ga is lower than that of bridged framework Al [28,29], resulting in a decreased density of strong acids. This can help prevent the formation of polycyclic aromatic hydrocarbons and inhibit coke deposition [30], thus improving the stability of the catalyst. In view of this, the high aromatic selectivity and stability in CO_2 assisted PDA reaction could be achieved over a catalyst that directly synthesized aluminum-free silica-gallium MFI zeolite using a one-step hydrothermal method.

Aside from introducing Ga to enhance the catalytic performance, the introduction of other metal elements as additives to Ga-based catalysts is also commonly employed [27,31–35]. Although the introduction of CO_2 to the feedstocks can partially assist in eliminating deposited coke via the reverse Boudouard reaction ($CO_2 + C \rightarrow 2CO$) [10], its effectiveness is limited due to the low conversion of CO_2. Considering the high chemical inertness of CO_2, the introduction of a second metal ingredient that can facilitate CO_2 activation, the elimination of hydrogen produced during the reaction should be simultaneous improved through the reverse water gas shift (RWGS) reaction ($CO_2 + H_2 \rightarrow CO + H_2O$), thus leading to the suppressed hydrogenation of intermediates for aromatization as well as the improved performance of the catalyst. Fan et al. demonstrated, through theoretical calculations, that the incorporation of Pt or Cu into the Zn/ZSM-5 catalyst can introduce additional active sites for aromatization, enhance the catalyst's ability through reducing the barrier of reverse Boudouard reaction, and facilitate the activation of CO_2 and elimination of coke precursors [36]. These findings suggest that such modifications can effectively improve the catalyst stability. Zhou et al. prepared a trimetallic catalyst, $Zn_{1.0}Fe_{0.3}Pt_{0.1}$/HZSM-5, by sequentially impregnating Fe and Pt onto a Zn/ZSM-5 catalyst. In comparison to Zn/ZSM-5, $Zn_{1.0}Fe_{0.3}Pt_{0.1}$/HZSM-5 exhibited much lower dry gas (CH_4 and C_2H_6) production, higher propane transformation activity, and improved BTX selectivity. The exceptional performance of this trimetallic catalyst was found to be attributed to the highly dispersion of the metals and the formation of FePt bimetallic dehydrogenation active sites, that will promote H atom recombination and desorption on the $[Zn\text{-}O\text{-}Zn]^{2+}$ sites by FePt sites [31]. Currently, there has been numerous researches on the introduction of a second active component as promoter in Zn/ZSM-5 catalysts, while the exploration in Ga-modified MFI catalysts is relatively deficient.

Above all, in order to improve the dispersion of Ga and its interaction with the zeolite framework, as well as to enhance the stability and aromatics selectivity of the catalyst, the H-type Ga-MFI zeolite without aluminum were synthesized through a straightforward one-step hydrothermal method. Additionally, for selecting the optimal metal promoter to improve the activity of Ga-MFI catalyst, the Fe, Co, Cu, Zn, and Pt as modifiers supported on Ga-MFI were prepared (M/Ga-MFI, M = Fe, Co, Cu, Zn, or Pt). The performance evaluation of the series catalysts in CO_2-PDA reaction revealed that Ga-MFI showed a better stability by comparing with Ga/Z5. In addition, Cu/Ga-MFI exhibited the highest aromatics selectivity, and the aromatics selectivity was as high as 73% at a propane conversion of 93.6%. NH_3-TPD, Py-IR, CO_2-TPD, in situ DRIFTs, DFT and other characterization methods were applied to gain insights into the relationship between the physicochemical properties and catalytic performance of the synthesized catalysts. The impact of copper on the catalyst performance was investigated, and the promotion mechanism of CO_2 in the dehydrogenative aromatization of propane was elucidated. This study offers a viable exploration strategy for design of high efficiency catalyst in CO_2-PDA.

2. Experiments

2.1. Catalyst preparation

2.1.1. Materials

All the chemicals, namely tetrapropylammonium hydroxide (TPAOH), tetraethyl orthosilicate (TEOS), aluminium isopropoxide ($Al(OCH_2CH_2CH_3)_3$), gallium nitrate hydrate ($Ga(NO_3)_2{\cdot}xH_2O$), ferric nitrate nonahydrate ($Fe(NO_3)_2{\cdot}9\ H_2O$), cobaltous nitrate hexahydrate ($Co(NO_3)_2{\cdot}6\ H_2O$), cupric nitrate trihydrate ($Cu(NO_3)_2{\cdot}3\ H_2O$), zinc nitrate hexahydrate ($Zn(NO_3)_2{\cdot}6\ H_2O$), platinum nitrate ($Pt(NO_3)_2$) solution (Pt,18.02 wt%), were used directly without further purification. The deionized water was obtained through an ultra-pure water system (RephiLe Bioscience, Ltd., 18.2 MWcm at 298 K).

2.1.2. Preparation of Ga-MFI and Al-MFI catalysts

The Ga-MFI zeolite was prepared by hydrothermal method. TPAOH was used as the template, the silicon source was TEOS and the Gallium source was $Ga(NO_3)_2{\cdot}xH_2O$. Typically, TPAOH (43.93 g) and Ga $(NO_3)_2{\cdot}xH_2O$ (2.48 g) were mixed with deionized water (100 mL) under vigorously stirring at 25 °C until the $Ga(NO_3)_2{\cdot}xH_2O$ is completely dissolved. Then TEOS (41.67 g) was slowly added into the above mixed solution. The mixture was kept stirring at 25 °C for 16 h, which was then heated in an oil bath at 85 °C for 4 h to evaporate the ethanol due to the hydrolysis of TEOS. Then deionized water were add to the above solution until the total volume was 125 mL, and the mixture was transferred into a 200 mL Teflon-lined stainless-steel autoclave for hydrothermal treatment at 170 °C for 72 h. After that, the solid was collected by centrifugation and washed by deionized water, and dried at 70 °C overnight. Then, the sample was calcined at 600 °C for 6 h to obtained the Ga-MFI.

The preparation of Al-MFI (Z5) catalysts were similar to that of Ga-MFI, simply by replacing the $Ga(NO_3)_2{\cdot}xH_2O$ with $Al(OCH_2CH_2CH_3)_3$, and adjusting the amount of $Al(OCH_2CH_2CH_3)_3$ appropriately.

2.1.3. Preparation of Metal/Ga-MFI (Metal = Fe, Co, Cu, Zn, Pt) catalysts

The Metal/Ga-MFI catalyst was prepared by a wet impregnation method, in which the content of metal is 3 wt%. A suspension containing a certain amount of deionized water, Ga-MFI zeolite and metal nitrates was kept stirring at 35 °C until the water was evaporated away. Then, the residue was dried overnight at 70 °C. Finally, the collected powder was calcined in air at 550 °C for 4 h, denoting as Metal/Ga-MFI (Metal = Fe, Co, Cu, Zn, Pt).

2.1.4. Preparation of Ga/Z5 and CuGa/Z5 catalysts

Ga/Z5 were prepared as follow: a suspension containing a certain amount of deionized water, Z5(SiAl = 69 , calculated from ICP-AES results) zeolite and $Ga(NO_3)_2{\cdot}xH_2O$ was kept stirring at 35 °C until the water was evaporated away. Then, the residue was dried overnight at 70 °C. Finally, the collected powder was calcined in air at 550 °C for 4 h, denoting as Ga/Z5 (the content of Ga is 2 wt%).

The preparation of CuGa/Z5 catalysts were similar to Ga/Z5, simply by replacing the Z5 with the Ga/Z5. The content of Cu in CuGa/Z5 is 3 wt%.

2.2. Catalysts characterization

Transmission electron microscopy (TEM), high-resolution transition electron microscopy (HRTEM) and high-angle annular dark-field scanning transmission electron microscopy (HAADF-STEM) images were carried out on a Tecnai G2 F20 S-Twin microscope equipped with an element mapping technique (SDD, X-max 80 T, OXFORD Instruments). Scanning electron microscope (SEM) images were carried out on Gemini 500 (Zeiss, Oberkochen, Ostalbkreis, Baden-Württemberg, Germany). X-ray diffraction (XRD) was performed using a Bruker D8 Advance X-ray diffractometer with the Ni-filtered Cu Kα radiation. The unit cell parameters were calculated by the Rietveld refinement method, using PC-GSAS software with an EXPGUI graphical interface, where the parameters were refined based on the unit cell. Nitrogen adsorption-desorption measurements were measured on an AUTOSORB-IQ (Quantachrome). The acidity of the catalysts was analyzed by the NH_3 temperature-programmed desorption (NH_3-TPD) and pyridine Fourier-transform infrared (Py-IR) spectrometer. NH_3-TPD were measured on the Micromeritics AutoChem II 2920. Before the NH_3-TPD test, 0.080 g catalysts were heated at 500 °C for 120 min under He flow (30 $mL{\cdot}min^{-1}$). When it cooled to 80 °C, a 30 mL/min NH_3 gas flow was introduced for 90 min. After that, the physical absorbed NH_3 was removed using He flow for 120 min. Py-IR spectra were collected under vacuum condition at 450 °C after pyridine desorption 30 min using a Bruker Invenio S instrument Fourier-transform infrared (FT-IR) spectrometer. Inductively coupled plasma-atomic emission spectrometry (ICP-AES) was performed on a PerkinElmer Optima 8000. ^{71}Ga MAS NMR (^{71}Ga magic-angle spinning nuclear magnetic resonance) experiments were performed on a Bruker AVANCE III 400 WB spectrometer at a resonance frequency of 122.13 MHz. The chemical shifts of ^{71}Ga were referenced to $Ga(NO_3)_3$. Thermogravimetric (TG) and differential scanning calorimetry (DSC) analyses were measured on Simultaneous Thermal Analyzer (Simultaneous DSC/TGA Discovery SDT 650) from 25 to 900 °C at a ramping rate of 10 °C min^{-1} under an oxidative atmosphere to analyze the weight and the degree of graphitization of coke on the spent catalysts. In situ diffuse reflectance infrared Fourier transform spectroscopy (in situ DRIFTs) experiments was measured on a Nicolet 6700 spectrometer with a mercury-cadmium-telluride detector and the resolution is 4 cm^{-1}. For all the DRIFTs experiments, the catalysts were firstly purged with He at 600 °C for 30 min and the flow rate was 50 $mL{\cdot}min^{-1}$. In the CO_2 hydrogenation, the catalysts were exposed to CO_2, H_2 and He (CO_2: H_2: He = 3: 0.6: 56.4 $mL{\cdot}min^{-1}$) at 600 °C and the spectra were collected.

2.3. Catalytic performance evaluation

The CO_2-PDA reaction was conducted in a home-made fixed-bed reaction system, in which the reactor was lined with a quartz tube. Typically, 0.3 g catalyst was packed in a quartz tube (4 mm inner diameter). Prior to each reaction, the catalyst was heated in the pure N_2 at 600 °C for 1 h with a gas flow of 40 $mL{\cdot}min^{-1}$ at 1 atm. The feedstocks (C_3H_8: CO_2: N_2 = 3: 3: 4 $mL{\cdot}min^{-1}$) were fed into the reactor at 600 °C at 1 atm with a gas hourly space velocity (WHSV) of 2000 $mL{\cdot}g_{cat}^{-1}{\cdot}h^{-1}$. The PDA reaction was conducted under similar conditions to the CO_2-PDA except the addition of CO_2 (the feedstocks were C_3H_8: N_2 = 3: 7 $mL{\cdot}min^{-1}$).

Two online gas chromatographs were employed for analysis of the products. One was equipped with a thermal conductivity detector (TCD) and a flame ionization detector (FID) for the gaseous products analysis. A 13X packed column (3 m × 3 mm O.D. × 3 mm I.D.) with a pre-linked Porapak Q packed column (2 m × 3 mm O.D. × 2 mm I.D.) was connected to the TCD, while a PoraPLOT Q capillary column (50 m × 0.32 mm × 10 μm) was connected to the FID. The other one was equipped with an FID and an FFAP capillary column (30 m × 0.32 mm × 1.0 μm), which was used to analyze all hydrocarbon products including aromatic products. The C_3H_8 conversion (C_{C3H8}), CO_2 conversion (C_{CO2}) and hydrocarbon selectivity (S_{CnHm}), were calculated according to the equations shown below:

$$C(C_3H_8) = \frac{C_3H_{8in} - C_3H_{8out}}{C_3H_{8in}} \times 100\%$$

$$C(CO_2) = \frac{CO_{2in} - CO_{2out}}{CO_{2in}} \times 100\%$$

$$S(C_nH_m) = \frac{n \times C_nH_{mout}}{\sum n \times C_nH_{mout}} \times 100\%$$

where C_3H_{8in}, CO_{2in} denote the moles of C_3H_8, CO_2 in the feedstock, and C_3H_{8out}, CO_{2out} and C_nH_{mout} denote the carbon moles of C_3H_8, CO_2 and C_nH_m at the outlet of the reactor, respectively.

3. Results and discussion

3.1. Catalytic performance

The catalytic performance of series catalysts were evaluated for CO_2-PDA reaction at 600 °C and 1 atm. Firstly, the differences between Al and Ga in the MFI framework in catalytic performance was compared by the catalyst evaluation of Z5 and Ga-MFI. As shown in Fig. 1 and Table 1, after 1 h CO_2-PDA reaction, the propane conversion of Z5 and Ga-MFI are 77.1% and 84.5%, respectively, and the aromatics selectivity (aromatics yield) of Z5 and Ga-MFI are 14.6% (11.9%) and 66.9% (59.6%). This demonstrated a better initial activity and superior aromatics selectivity can be achieved on Ga-MFI zeolite, which can be attributed to the distinct acidity and dehydrogenation ability caused by the introduction of Ga. According to the literature, the acidic sites presented in ZSM-5 catalysts show a poor dehydrogenation ability, but are more prone to catalyze the C-C bond cleavage of propane, leading to the predominant formation of methane and ethylene as the main products [12,13,36]. In contrast, Ga-MFI has exhibited a better dehydrogenation ability, favoring the cleavage of C-H bonds in propane. Consequently, it will promote the production of alkenes, which as intermediates subsequently undergo oligomerization on the acidic sites within the pores of Ga-MFI to generate aromatics. As result, the main products in Ga-MFI are aromatics.

In order to distinguish the difference in catalytic performance of Ga within and outside the MFI framework, considering that the acid-free pure-silica MFI zeolite (Silicalite-1) may lead to poor aromatization

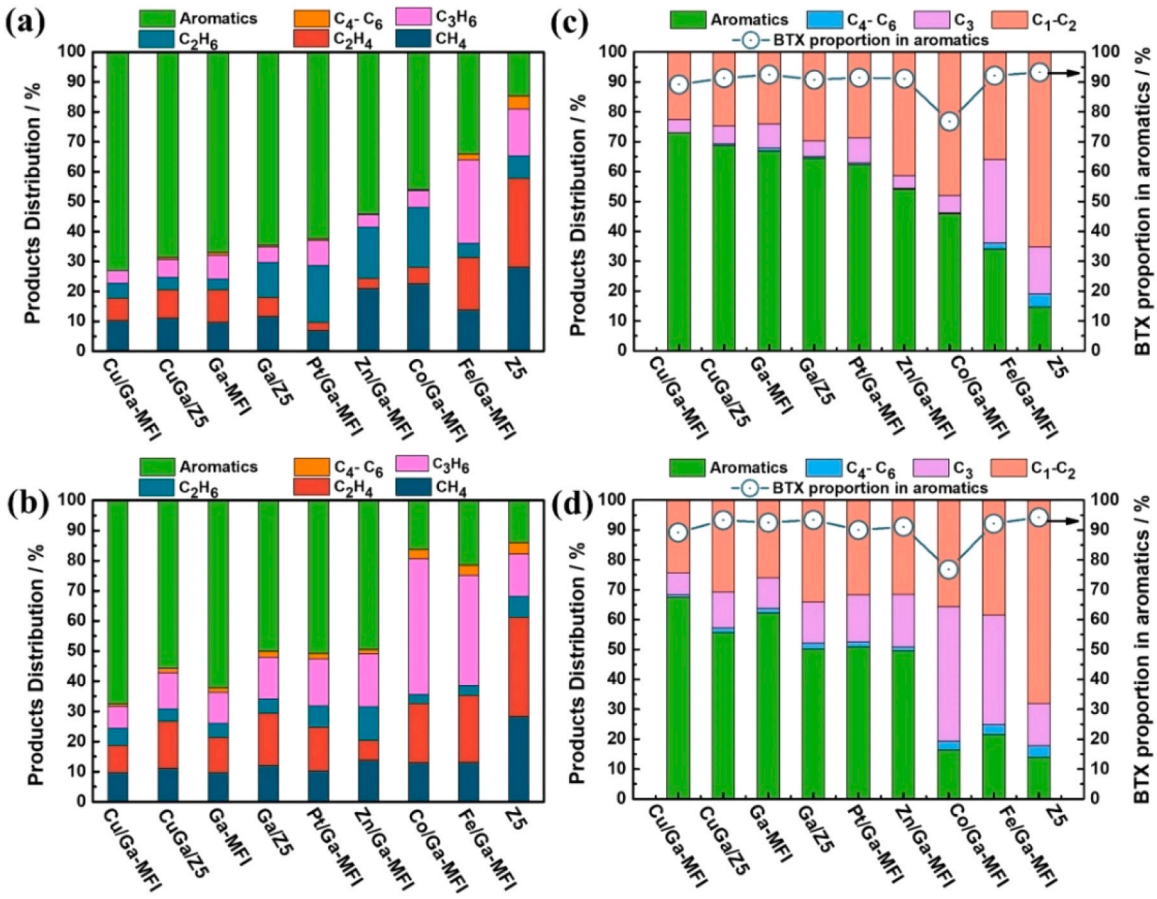

Fig. 1. Hydrocarbon products distribution after (a) 1 h; (b) 10 h; Hydrocarbon products distribution and the BTX proportion in aromatics after (c) 1 h; (d) 10 h of different catalysts for the CO_2-PDA reaction. (C_4-C_6 = non-aromatic hydrocarbon containing 4–6 carbon atoms; C_1-C_2 = CH_4 + C_2H_4 + C_2H_6; BTX = aromatic compounds containing 6–8 carbon atoms.) Experimental conditions: 0.3 g Catalysts (40–60 mesh); 600 °C; 1 atm; C_3H_8: CO_2: N_2 = 3: 3: 4 mL/min.

Table 1
Catalytic performance of different catalysts for CO_2-PDA.

Catalyst	Conversion (%)		Hydrocarbon products selectivity (%)						Aromatic yield (%)
	C_3H_8	CO_2	CH_4	C_2H_4	C_2H_6	C_3H_6	C_{4+}	Aromatics	
Cu/Ga-MFI	93.6	36.2	10.2	7.6	4.9	4.3	0.0	73.0	72.5
CuGa/Z5	87.2	33.6	11.1	9.5	4.1	6.0	0.6	68.7	63.7
Ga-MFI	84.5	27.6	9.6	10.9	3.6	8.0	1.0	66.9	59.6
Ga/Z5	90.9	33.5	11.6	6.5	11.6	5.2	0.6	64.5	61.8
Pt/Ga-MFI	94.9	47.2	7.0	2.6	19.0	8.4	0.6	62.4	58.8
Zn/Ga-MFI	97.3	49.3	21.0	3.4	17.0	4.2	0.2	54.2	49.6
Co/Ga-MFI	94.7	42.4	22.6	5.5	19.9	5.8	0.3	45.9	43.6
Fe/Ga-MFI	42.1	23.5	13.8	17.5	4.6	28.0	2.0	34.1	14.2
Z5	77.1	18.8	28.1	29.7	7.4	15.8	4.4	14.6	11.9

Reaction condition: 0.3 g catalyst (40–60 mesh); 600 ℃; 1 atm; C_3H_8: CO_2: N_2 = 3: 3: 4 mL/min; WHSV = 2000 mL·g^{-1}·h^{-1}; time on stream (TOS) = 1 h.

ability, we prepared Ga/Z5 by wet impregnation using ZSM-5 instead of Silicalite-1 as the support. For Ga/Z5, the propane conversion and the aromatics selectivity (aromatics yield) after 1 h CO_2-PDA reaction are 90.9% and 64.5% (61.8%), respectively. Moreover, the selectivity to dry gas (CH_4 and C_2H_6) for Ga/Z5 and Ga-MFI are 23.2% and 13.2%, respectively (Table 1). After 10 h reaction, the propane conversion of Ga/Z5 and Ga-MFI are 70.9% and 75.3%, respectively, and the aromatics selectivity (aromatics yield) of Ga/Z5 and Ga-MFI are 50.1% (37.2%) and 62.2% (49.8%), respectively (Table S1). Compared with Ga/Z5, Ga-MFI shows lower dry gas selectivity, higher stability and maintains higher aromatic selectivity over a period of 10 h CO_2-PDA reaction, although it gives a slightly lower initial activity, which may be ascribed to the lower acid strength of bridged framework Ga sites than that of bridged framework Al sites [28,29].

In order to enhance the catalytic activity of Ga-MFI, a second metal is employed as an additive. After being modified with different metals, the catalytic performance of M/Ga-MFI (M = Fe, Co, Cu, Zn, Pt) catalysts was evaluated for CO_2-PDA reaction. As shown in Fig. 1 and Table 1, a propane conversion of 93.6% with aromatics selectivity (aromatics yield) of 73.0% (72.5%) was achieved over Cu/Ga-MFI catalyst after 1 h on stream, giving the highest yield of aromatic products, while the propane conversion (aromatics selectivity) for Fe/Ga-MFI, Co/Ga-MFI, Zn/Ga-MFI and Pt/Ga-MFI were 42.1% (34.1%), 94.7% (45.9%), 97.3% (54.2%), and 94.9% (62.4%), respectively. By compared with Ga-MFI catalyst, it can be found that Co, Cu, Zn, or Pt modification could facilitate the conversion of C_3H_8. However, only Cu could further

enhance the aromatics selectivity (from 66.9% to 73.0%, Table 1), while loading of Co, Zn, and Pt on Ga-MFI led to a varying degree of decrease in aromatics selectivity. In addition, a decreased activity was found over Fe/Ga-MFI catalyst, and the propane conversion decreases from 94.7% to 38.2% over Co/Ga-MFI after 10 h, indicating a more severe deactivation, which could be ascribed to the rapid coke deposition. Moreover, by comparing with Ga/Z5, the addition of Cu (CuGa/Z5) resulted in an increase in aromatics selectivity from 64.5% to 68.7%, while propane conversion decreased from 90.9% to 87.2% after 1 h on stream (Table 1). On the other hand, after 10 h CO_2-PDA reaction, the conversion of propane over Cu/Ga-MFI catalyst showed a slight decrease of 5.9% from 93.6% to 87.7% with the selectivity to aromatics maintained above 67.5%. But for CuGa/Z5 catalyst, a reduction of 23.9% of the propane conversion from 87.2% to 63.3% was appeared, while the aromatics selectivity significantly decreased from 68.7% to 55.6% (Table 1 and Table S1). In view of above results, the Cu/Ga-MFI has exhibited a superior catalytic performance with the highest aromatics selectivity and reaction stability during the 10 h of CO_2-PDA reaction. Moreover, it is worth noting that the aromatic products of all the catalysts were mainly composed of BTX, accounting for approximately 90% (except for Co/Ga-MFI was approximately 80%) of the aromatics (Fig. 1c-d, Fig. S1, Table S2 and Table S3).

To investigate the effect of reaction temperature on the catalyst performance, the CO_2-PDA reaction of Ga-MFI and Cu/Ga-MFI were tested at different temperatures without changing the space velocity. As represented in Fig. 2a, the propane conversion over Ga-MFI catalyst

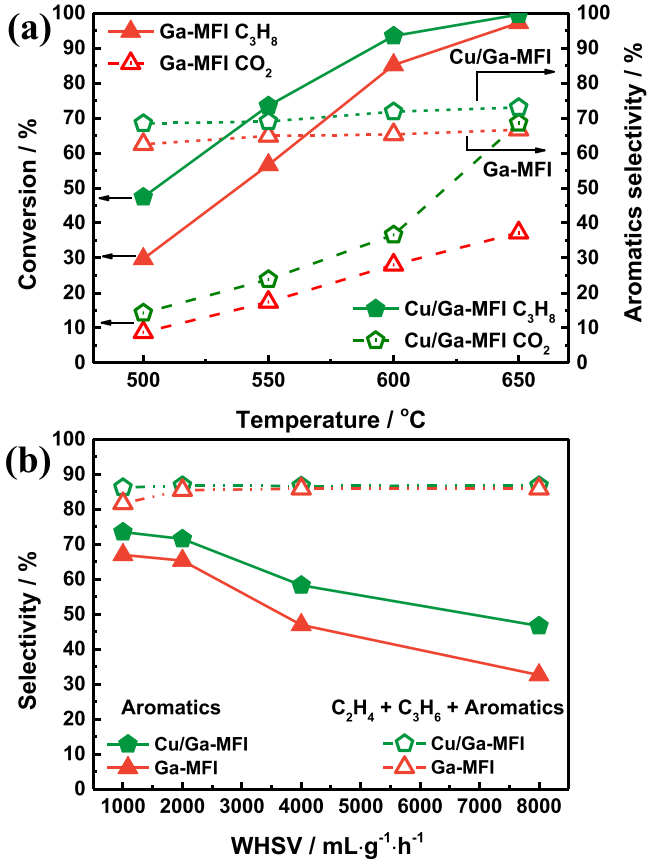

Fig. 2. (a) C_3H_8, CO_2 Conversion and aromatics selectivity of Ga-MFI (red) and Cu/Ga-MFI (green) at different reaction temperatures. Experimental conditions: 0.3 g Catalysts (40–60 mesh); 1 atm; C_3H_8: CO_2: N_2 = 3: 3: 4 mL/min; WHSV = 2000 mL·g^{-1}·h^{-1}; (b) aromatics, olefins and aromatics (C_2H_4 + C_3H_6 + aromatics) selectivity of Ga-MFI (red) and Cu/Ga-MFI (green) at different WHSV. Experimental conditions: 0.3 g Catalysts (40–60 mesh); 600 °C, 1 atm; C_3H_8: CO_2: N_2 (volume ratio) = 3: 3: 4.

increased from 29.8% to 97.2% as the reaction temperature was elevated from 500 °C to 650 °C with an increment of 50 °C, while the selectivity to aromatics had shown an increase from 62.5% at 500 °C to 66.7% at 650 °C. By contrast, after being modified with Cu, an improved catalytic performance of Cu/Ga-MFI catalyst had been achieved in the same range of reaction temperature as propane conversion increased from 47.5% to 99.6% and selectivity to aromatics increased from 68.4% to 73.0%, respectively. This indicates that raising the reaction temperature within a certain range is beneficial to improving the catalyst's activity and aromatics selectivity. Although there was a slight increase in the selectivity to heavier hydrocarbons with increasing temperature, the BTEX remained the dominant components in the aromatic products (Fig. S2). Meanwhile, the CO_2 conversion can also be enhanced by the introduction of Cu, giving a significant increase from 14.3% at 500 °C to 68.6% at 650 °C, of which an increase from 8.8% to 37.2% was received over Ga-MFI catalyst (Fig. 2a). A more pronounced variation in CO_2 conversion with increasing reaction temperature can be found on Cu/Ga-MFI, which may be attributed to the better promotion of CO_2 adsorption and activation induced by the introduction of Cu to the Ga-based surface acidic sites, thus facilitating the RWGS reaction for elimination of the produced hydrogen [36].

The effect of weight hourly space velocity (WHSV) on catalyst performance was further investigated while maintaining the reaction temperature at 600 °C, and the results are illustrated in Fig. 2b and Fig. S3. The conversion of propane and CO_2 as well as the selectivity to aromatics showed a downtrend on both Ga-MFI and Cu/Ga-MFI catalysts with the increased WHSV (Fig. S3). For Ga-MFI, it can be found that the conversion of propane and selectivity to aromatics decreased dramatically from 91.7% and 67.0% at WHSV of 1000 mL·g^{-1}·h^{-1} to 31.1% and 32.6% at WHSV of 8000 mL·g^{-1}·h^{-1}, giving a decrease by 60.6% in conversion and 34.4% in selectivity, respectively. However, a higher propane conversion of 65.2% with a 46.6% selectivity to aromatics can also be obtained on Cu/Ga-MFI at the WHSV of 8000 mL·g^{-1}·h^{-1}, showing a decrease by 34.7% and 26.9%, respectively, relative to that at WHSV of 1000 mL·g^{-1}·h^{-1}. These results have demonstrated the outstanding activity of Cu/Ga-MFI catalyst in CO_2-PDA reaction, and the significant boost of Cu to the conversion of propane as well as the aromatization of olefin intermediates. In addition, it should be noted that the selectivity to olefins increased as the decreasing selectivity to aromatics (Fig. S3), and the total selectivity to olefins and aromatics (C_2H_4 + C_3H_6 + aromatics) maintained over 81% on Ga-MFI and Cu/Ga-MFI catalysts with negligible variations observed across different WHSV (Fig. 2b), indicating that the prolonged residence time of reactants will favor the aromatization process. This means that within a certain range, the variation in WHSV has a limited impact on the rate of propane dehydrogenation to unsaturated hydrocarbons, whereas it exerts a significant influence on the subsequent aromatization of the resulting unsaturated hydrocarbons. In the aromatic products, the selectivity of heavier hydrocarbons also decreased with the increase of WHSV (Fig. S3).

3.2. Characteristics

3.2.1. Morphology analysis

The morphology of the synthesized catalysts was analyzed using scanning electron microscopy (SEM) and transmission electron microscopy (TEM) (Fig. 3 and Fig. S4). As shown in Fig. S4, both Ga-MFI and Ga/Z5 exhibited irregular crystal agglomerates, with Ga/Z5 having slightly larger average particle size ranging from 100 to 150 nm compared to Ga-MFI. The average particle size of copper oxide on the surface of Cu/Ga-MFI is found as approximately 2 nm (Fig. 3b). The crystal surface exhibited distinct lattice fringes (Fig. 3a and Fig. S4c), indicating good crystallinity. Moreover, the EDS mapping results demonstrated a relatively uniform distribution of Cu on the Ga-MFI zeolite (Fig. 3c-f).

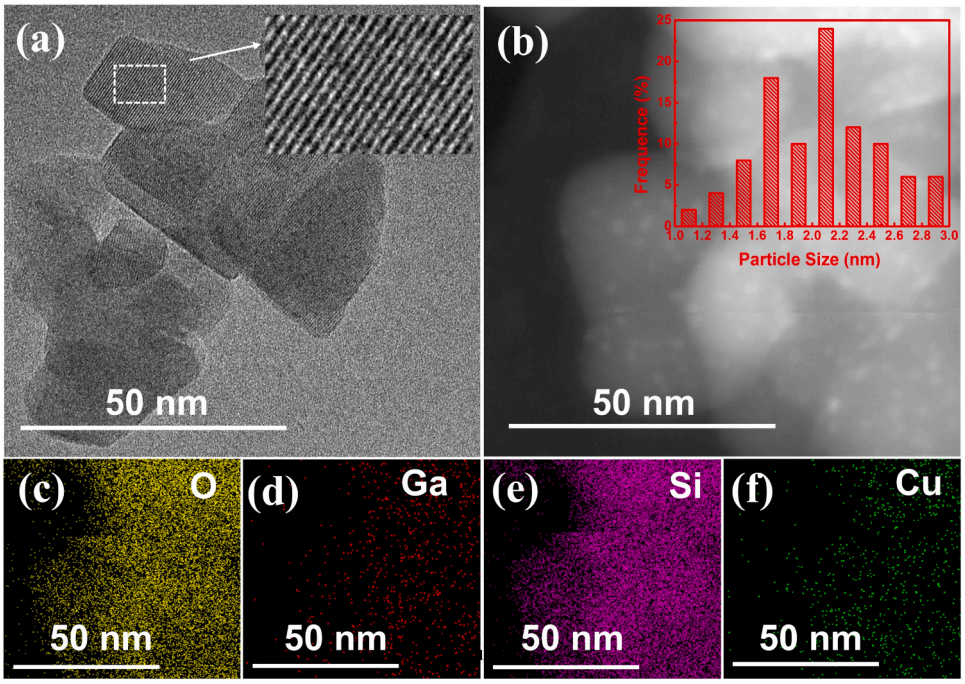

Fig. 3. (a) HRTEM; (b) HAADF-STEM and (c-f) EDS mapping images of Cu/Ga-MFI.

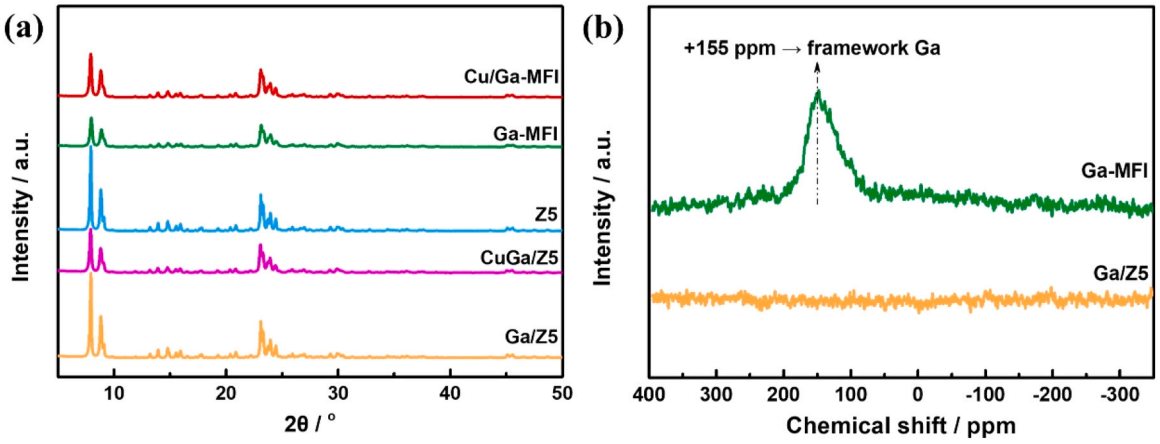

Fig. 4. (a) XRD) patterns; (b) ^{71}Ga MAS NMR spectrum for the catalysts.

3.2.2. Structural properties

The synthesized series of catalysts were characterized using X-ray diffraction (XRD), as shown in Fig. 4a and Fig. S5a. All catalysts exhibited typical MFI crystalline peaks, and the introduction of the second metal hardly impact on the crystal structure of the zeolite. No distinct characteristic peaks corresponding to the metal species were observed in the spectra, indicating the uniform distribution of the metals. In addition, considering the difference in ionic radius between Ga^{3+} (0.62 Å) and Al^{3+} (0.51 Å) ions, the XRD Rietveld refinement were investigated in order to distinguish the difference of crystal structures between Ga-MFI and Al-MFI (Z5) with same Si/Ga or Si/Al ratio. As shown in Fig. S6, a slight lattice expansion of Ga-MFI compared with Z5 was found, which can be attributed to the larger ionic radius of framework Ga in the zeolite [37].

In order to investigate the difference in the Ga state between framework Ga and supported Ga species in the zeolite, the Ga-MFI and Ga/Z5 catalysts were further characterized using ^{71}Ga magic angle spinning nuclear magnetic resonance (MAS NMR). As shown in Fig. 4b, the peak at + 155 ppm in Ga-MFI can be corresponded to the four-coordinated framework Ga species, confirming the successful incorporation of Ga into the zeolite framework. In Ga/Z5, Ga existed as extra-framework species, which lacked symmetry and was therefore difficult to detect, resulting in the absence of peaks in the spectrum [6]. In addition, the Ga-MFI and Ga/Z5 were treated by hydrochloric acid solution to remove the extra-framework species that weakly interacted with zeolite. The Ga content of samples after acid treatment was analyzed by ICP-AES. The mass percentage of Ga in Ga-MFI remained essentially unchanged (5.6 wt%) before and after HCl treatment, while that in Ga/Z5 was significantly decreased from 2.5 wt% to 0.8 wt% (Table S4). This result indicates that the Ga species located on the extra-framework (non-ionic exchange positions) of zeolite can be easily removed by HCl, while Ga cations in the zeolite framework or at the ion-exchange sites, due to their strong coordination stability, were difficult to remove. Combined with the XRD Rietveld refinement and the ^{71}Ga MAS NMR results, it has demonstrated that Ga had been successful incorporation into the MFI zeolite framework with no aggregated Ga species on the surface of Ga-MFI through the one-step hydrothermal method, which had exhibited higher coordination stability. This may

explain its higher activity and catalytic stability compared to Ga/Z5, which is consistent with the performance results of CO_2-PDA. On the other hand, in addition to copper oxide particles, Cu cations in the Cu/Ga-MFI could be identified through the OH-stretching region IR spectra. Compared with Ga-MFI, the equivalent intensities of the band at 3610 cm^{-1} and 3740 cm^{-1}, which could be corresponded to the bridging hydroxyls at Brønsted acid site and isolated terminal silanol groups, respectively, decreased for Cu/Ga-MFI (Fig. S7a). This could be attribute to the interaction between Cu species and the related -OH groups [38]. The -OH-stretching region IR results could indicate the presence of Cu cations in Cu/Ga-MFI, and according to the literature, a possible structure of Cu cations on the ion-exchange sites was proposed in Fig. S7b [39]. These Cu cations could act as Lewis acids and also contribute to the heterolytic cleavage of a C-H bond of propane.

The textural properties and elemental compositions of each catalyst are represented in Fig. S5b, Fig. S5c, Table 2, and Table S5. N_2 adsorption-desorption isotherms (Fig. S5b and Fig. S5c) indicate that all catalysts exhibited a typical composite structure of micropores and mesopores, of which the mesopores were mainly originated from voids between the aggregated zeolite crystals (Fig. S4c and Fig. S4d). After with metal modification, the surface area, and micropore volume of Z5 and Ga-MFI decreased (Table 2 and Table S5). XPS results reveal that the surface Si/Ga ratio in Ga-MFI (17) remains higher than that in Ga/Z5 (12), even when the overall Ga content in Ga-MFI is significantly higher than Ga/Z5 (Table 3). These results support the notion that Ga species in Ga/Z5 are primarily located on the external surface of Z5. However, it can be found that Cu ions can penetrate the zeolite channels after Cu impregnation, because a notable decrease in micropore surface area and micropore volume was exhibited on CuGa/Z5 (from 434 m^2/g and 0.19 cm^3/g to 305 m^2/g and 0.14 cm^3/g, respectively) and Cu/Ga-MFI (from 410 m^2/g and 0.18 cm^3/g to 351 m^2/g and 0.15 cm^3/g, respectively). Furthermore, the surface and bulk content of Cu on the samples were detected by XPS and ICP, respectively. As shown in Table 3, a higher content difference of 0.7% (3.2% vs 3.9%) is obtained on Cu/Ga-MFI, compared to that of 0.2% (4.0% vs 4.2%) on CuGa/Z5. This shows that Cu species had a distribution in the pore channels of zeolite for both CuGa/Z5 and Cu/Ga-MFI, and a higher content of Cu in the micropores was achieved in Cu/Ga-MFI, which could contribute to the aromatization of olefin intermediates during the CO_2-PDA reaction [40].

3.2.3. Acid properties

The acidity of the catalysts was analyzed using NH_3 temperature-programmed desorption (NH_3-TPD) and pyridine infrared spectroscopy (Py-IR). As shown in Fig. 5 and Table 3, the NH_3 desorption peaks of chemisorbed ammonia at 168 and 364 °C can be observed on Z5, while peaks at 168 and 340 °C appear on Ga-MFI. Compared to Z5, Ga-MFI shows a shift of peak temperatures towards lower temperatures (Fig. 5a), indicating a relatively weaker acidity when Al atoms in the zeolite framework were replaced with Ga. This could be attributed to the larger electronegativity difference between Si and Al compared to Si and Ga. Consequently, the acidity of the unit B acid site formed by Al in the framework is stronger than that formed by Ga in the framework, which is consistent with previous literature reports [28,29]. After Ga loading, the strength and total content of acid sites on Ga/Z5 significantly decreased (from 0.63 to 0.51 mmol·g^{-1}), primarily due to two factors. Firstly, in order to ensure similar content of active metal components in the catalysts, a zeolite with a higher Si/Al ratio was chosen as the support for Ga/Z5 (SiAl = 69 (66/0.96), Si/(Al+Ga) = 34), as compared to the Si/Al ratio of 40 for Z5 (Table 3). Secondly, Ga species covered a portion of the strong acidic sites on Z5 during the preparation, where GaO_x particles were simultaneously formed. Moreover, the subsequent impregnation of Cu on Ga/Z5 or Ga-MFI resulted in the disappearance of peaks at 352 °C or 340 °C and the appearance of a new desorption peak at 228 °C or 231 °C. This can be attributed to the penetration of Cu into the zeolite channels and the exchange of B acidic proton with Cu ions, leading to the formation of new medium-strength acid sites [41]. Furthermore, the desorption peak observed above 400 °C can be attributed to NH_3 adsorption at the strong L acid sites formed by non-ionic exchange Cu species for both CuGa/Z5 and Cu/Ga-MFI [38,40,42,43]. This strong L acid may facilitate the dehydrogenation of propane, and thus enable Cu/Ga-MFI catalyst a superior activity with improved propane conversion.

Comparing the Py-IR results of Z5 and Ga-MFI, when Ga located in the MFI zeolite framework, the proportion of B acid in Ga-MFI is lower than that in Z5 with Al in the framework, and a contrary tendency can be found for the proportion of L acid (Table 3, Fig. 5b). As a result, the B/L ratio in Z5 (B/L = 4.2) is approximately 1.56 times higher than that of Ga-MFI (B/L = 2.7). Previous studies indicate that the maximum attainable Ga content in silicon-rich gallosilicate zeolites framework is generally lower than the Al content in comparable aluminosilicate structures, and the strength of the acidity of B acid contribute from the bridged framework Ga is lower than that of bridged framework Al [29]. In addition, when the Si/Ga ratio in Ga-MFI is relatively low, high temperatures will tend to facilitate the detachment of Ga from the zeolite framework [6,28]. And the synergy between Ga species and its adjacent B acid sites is crucial for highly efficient and selective oligomerization of olefins [44,45]. Therefore, moderate acid strength with an appropriate B/L ratio in Ga-MFI may be the main reasons for its high aromatic selectivity and stability.

Moreover, the Py-IR results of Cu/Ga-MFI, CuGa/Z5, Ga-MFI and Ga/Z5 have shown that the introduction of Cu leads to a significant decrease in the B/L ratio, with the generation of numerous strong L acid sites in Cu/Ga-MFI and CuGa/Z5. As shown in Table 3, compared with Ga-MFI and Ga/Z5, the B/L ratio both decreased from 2.71 to 0.12 or 0.09 for Cu/Ga-MFI or CuGa/Z5, respectively. The results indicate that there was a higher proportion of ionic exchanged Cu species in CuGa/Z5 than Cu/Ga-MFI. Combined with the NH_3-TPD results, the acid content at 231 °C of Cu/Ga-MFI (0.41 mmol·g^{-1}) is lower than that at 228 °C of CuGa/Z5 (0.53 mmol·g^{-1}), which is in accordance with the Py-IR result. The NH_3-TPD and Py-IR analysis, combined with the pore structure data and the elemental analysis of catalysts (Table 2), could indicate that

Table 2
Specific surface area and pore volume of different samples.

Catalyst	Surface area (m^2/g)			Micropore volume[b] (cm^3/g)
	Total[a]	Micro-[b]	External[b]	
Z5	557	435	122	0.20
Ga/Z5	532	434	98	0.19
CuGa/Z5	387	305	82	0.14
Ga-MFI	539	410	129	0.18
Cu/Ga-MFI	465	351	114	0.15

[a] Determined by BET method.
[b] Determined by t-plot method.

Table 3
Chemical composition, ratio of Brønsted acid to Lewis acid (B/L), and acid content from NH_3-TPD for each catalyst.

Catalyst	Si/Al/Ga[a]		Cu Content (wt%)		B/L[b]	acid content (mmol·g^{-1})[c]		
	ICP	XPS	ICP	XPS		1	2	3
Z5	40/1/0	/	/	/	4.22	0.34	0.29	/
Ga-MFI	39/0/1	17/0/1	/	/	2.71	0.34	0.28	/
Cu/Ga-MFI	29/0/1	/	3.9	3.2	0.12	0.13	0.41	0.26
CuGa/Z5	73/1.01/1	/	4.2	4.0	0.09	0.18	0.53	0.02
Ga/Z5	66/0.96/1	22/1/1.83	/	/	2.71	0.28	0.23	/

[a] calculated from ICP-AES or XPS results (molar ratio).
[b] Obtained from the Py-IR (Area ratio).
[c] Obtained from the NH_3-TPD.

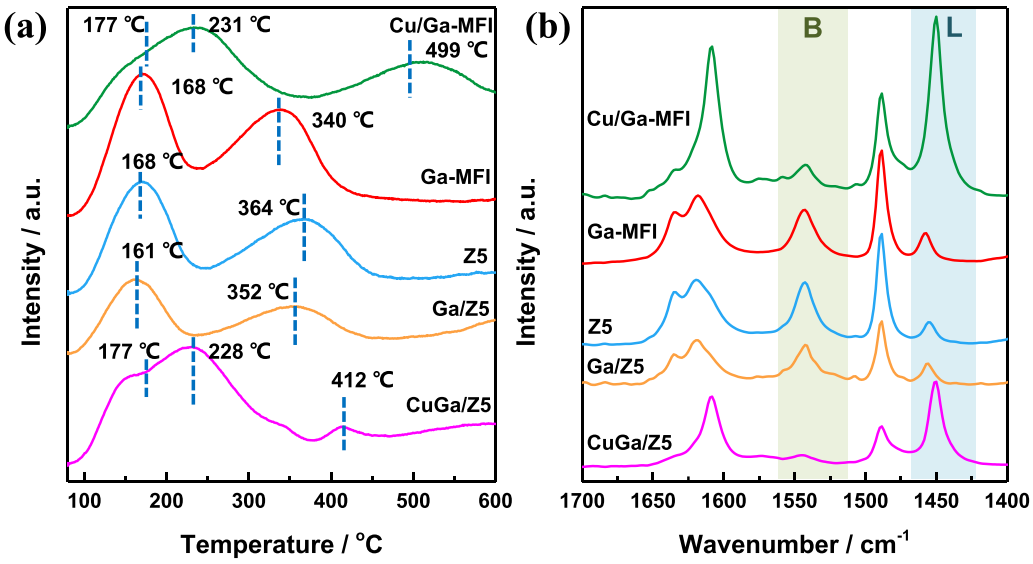

Fig. 5. (a) NH_3-TPD profiles and (b) Py-IR spectrum (collected after 30 min of isothermal treatment at 450 °C) of each catalyst.

there were more strong L acid sites formed by non-ionic exchange Cu species with a higher distribution in the channels of Cu/Ga-MFI. These well distributed strong L acid sites adjacent to the B acid sites not only enhance the activity of the catalyst but also synergistically promote rapid oligomerization and cyclization-dehydrogenation of olefins, thus improving aromatics selectivity [13,18,46]. Therefore, the introduction of Cu results in a significant enhancement of both activity and aromatic selectivity in Cu/Ga-MFI.

3.3. Density function theory

Density function theory (DFT) was implemented to reveal the high activity and selectivity of propane aromatization on Ga-MFI (The computational details were shown in Supplementary Material). As a comparison, the pristine Z5 was also investigated, where a hydrogen atom is added to the oxygen on zeolitic framework near the active-site metal (Al or Ga) to construct the Brønsted acid site on both Z5 and Ga-MFI zeolite. Generally, the first step of the C-H bond breaking of propane is an activity indicator of propane activation. Generally, the first and the second C-H bond breaking steps of propane ($C_3H_8 \rightarrow C_3H_7$ and $C_3H_7 \rightarrow C_3H_6$) are the activity indicators of propane activation. We have considered both propane dehydrogenation (PDH) and oxidative dehydrogenation of propane (ODHP) pathways, as shown below.

$$C_3H_8^* \rightarrow C_3H_7^* + H^* \rightarrow C_3H_7^* + \frac{1}{2}H_2(g) \rightarrow C_3H_6^* + H^* + \frac{1}{2}H_2(g) \rightarrow C_3H_6^* + H_2(g) \quad (1)$$

$$C_3H_8^* + 2OH^* \rightarrow C_3H_7^* + OH^* + H_2O \rightarrow C_3H_6^* + 2\,H_2O \quad (2)$$

Our results show that PDH is more favorable than ODHP pathway (Fig. S8). In the following, we only focus on the PDH pathway.

As shown in Fig. 6, firstly, propane adsorbs onto Z5 at an exothermic of − 0.63 eV, consistent with the literature [36]. Next, two modes of C-H activation of propane are considered, namely the cleavage of the central or the terminal C-H bond of propane. Our calculations show that energy change (ΔE) for the for the cleavage of the central and terminal C-H

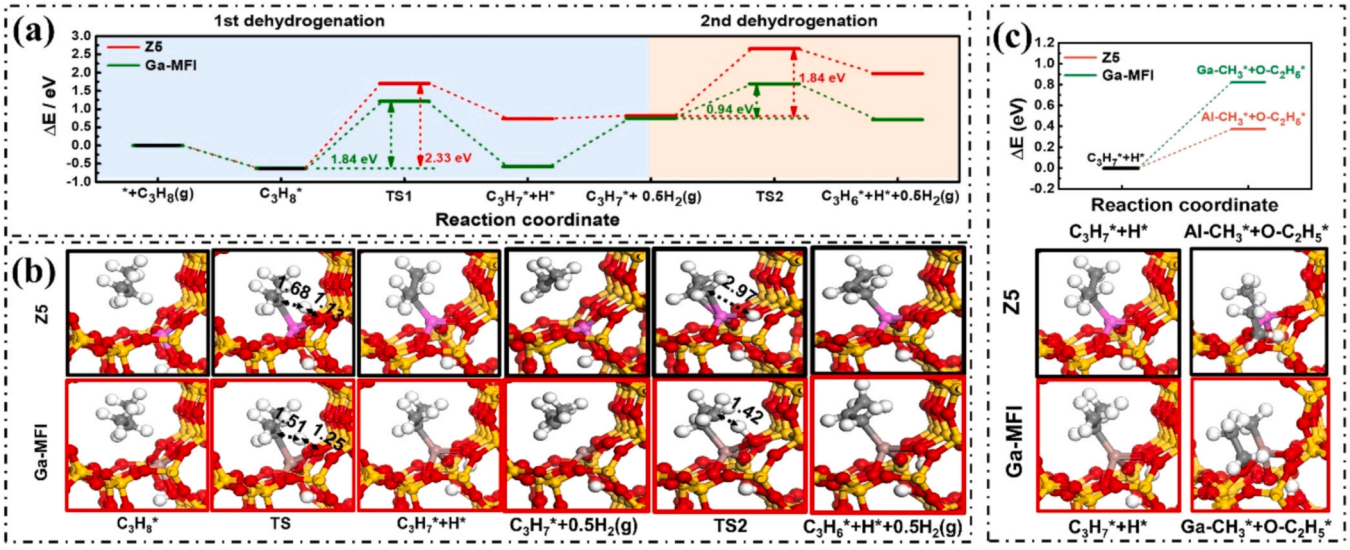

Fig. 6. (a) Energy profile of the first and second dehydrogenation of propane on Z5 and Ga-MFI, respectively; (b) The corresponding atomic structure of the first and second dehydrogenation of propane on Z5 and Ga-MFI, and (c) Thermodynamic energy changes of C-C cleavage on Z5 and Ga-MFI in methyl-bonded to metal sites (Al/Ga-CH_3 *+O-C_2H_5 *) mode and the corresponding atomic geometries.

bond are + 0.81 eV and + 2.07 eV, respectively (Fig. S9) indicating the cleavage of the central C-H bond is thermodynamically more favorable on Z5. Accordingly, the C-H activation on Z5 follows the cleavage of the central C-H bond, and the energy barrier for central C-H cleavage is 2.33 eV on Z5, resulting in the C_3H_7 * +H* intermediate (Fig. 6). Then, the adsorbed hydrogen atom (H*) on Z5 can be removed from the surface, which is endothermic of 0.08 eV. In the second C-H bond breaking step, the energy change is + 1.16 eV, with an energy barrier of 1.84 eV. Altogether, the second C-H bond breaking step is the rate-determining step for propane to propene on Z5.

For the Ga-MFI, the adsorption of propane is exothermic of − 0.62 eV (similar to that of Z5) and exhibits the same central C-H bond cleavage mode (+0.04 eV) as shown in Fig. S10 (cf. ΔE for the terminal C-H bond cleavage is +1.36 eV). Notably, the energy barrier for central C-H cleavage on Ga-MFI (1.84 eV) is lower than that on Z5 (2.33 eV). Then, the adsorbed hydrogen atom is removed from the surface, with an energy change of + 1.33 eV. In the second C-H bond breaking step, the energy change is − 0.05 eV, with an energy barrier of 0.94 eV. Therefore, the second C-H bond breaking step is the rate-determining step for propane to propene on Ga-MFI.

By comparing the energetic profiles on both Z5 and Ga-MFI, we can find that the energy barriers for two C-H bond breaking steps on Ga-MFI (1.84 and 0.94 eV) are lower than that on Z5 (2.33 and 1.84 eV). Accordingly, the C-H bond lengths of the transition state (TS1 and TS2, Fig. 6b) at the Ga-O site are 1.51 and 1.42 Å, shorter than that of TS at the Al-O site (1.68 Å and 2.97 Å, Fig. 6b). As a result, the overall barrier (TS2 to C_3H_8 *) on Ga-MFI is 2.32 eV lower than that on Z5 (3.29 eV). All results suggest that the propane activation on Ga-MFI is superior to that on Z5.

In addition, the ΔE for the C-C cleavage of propane to CH_3 * +C_2H_5 * was also investigated, which determines the tendency of side reaction toward CH_4. A lower (more negative) ΔE indicates the higher selectivity toward CH_4. For this purpose, we consider both the methyl-bonded metal site (Al/Ga-CH_3 *+O-C_2H_5 *) and the ethyl-bonded metal site (O-CH_3 *+Al/Ga-C_2H_5 *) configurations. The results show that ΔE for the C-C cleavage of propane on Z5 is at least 0.1 eV lower than that on Ga-MFI (see Fig. 6c and Fig. S11), regardless of the methyl-bonded to metal sites or ethyl-bonded to metal sites configurations. This result indicates that the Ga-MFI can suppress the C-C cleavage of propane.

The DFT results were consisted with the catalytic performance and literatures [12,13,36]. It has proved that the acid sites present in Z5 catalysts shown a poor dehydrogenation ability, which were more prone to catalyze cleavage the C-C bond in propane, leading to the main products were methane and ethylene. However, Ga-MFI has a better dehydrogenation ability, favoring the cleavage of C-H bonds in propane. This promotes to produce alkenes, which subsequently undergo oligomerization on the acidic sites within the pores of Ga-MFI to generate aromatics. The products in Ga-MFI are mainly aromatics.

Combined with the catalytic performance, structural properties, acid properties and DFT results, we may conclud that the uniformly dispersed Ga species synergy between its adjacent B acid sites in the framework of Ga-MFI, which can enable stronger interactions between Ga and zeolite, and facilitate the formation of alkene intermediates as well as the aromatization process, thus improving aromatics selectivity and catalytic stability. These highly dispersed Ga species can not only assist in propane dehydrogenation but also provide suitable acidity and inhibit the excessive polymerization of aromatic precursors during the aromatization process. In Ga/Z5, Ga mainly dispersed on the surface of ZSM-5, resulting in a long distance between the dehydrogenation site and the active site for olefin-intermediate polymerization. Furthermore, the strong acidity presented in the ZSM-5 channels will promote the undesired polymerization of aromatic precursors, resulting in the formation of heavy hydrocarbons as well as the deposited carbon that can clog the pores. Therefore, despite having higher initial catalytic activity, Ga/Z5 is more prone to deactivation due to carbon accumulation compared to Ga-MFI, leading to poor stability.

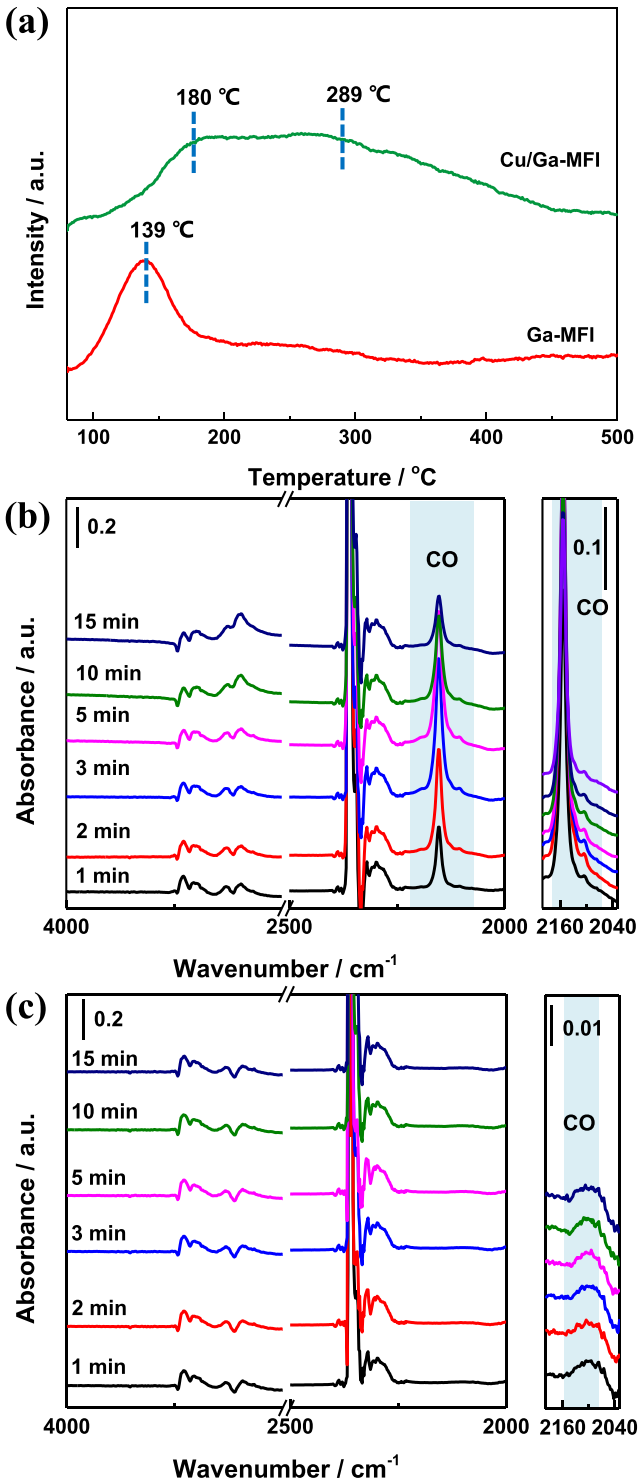

Fig. 7. (a) CO_2-TPD profiles of Ga-MFI and Cu/Ga-MFI; In situ DRIFTs spectrum of (b) Cu/Ga-MFI and (c) Ga-MFI for CO_2 activation with H_2.

3.4. Discussion on possible role of Cu

To further investigate the influence of Cu on the adsorption and activation of CO_2, CO_2-TPD and in situ DRIFTs were utilized (Fig. 7). From Fig. 7a, it can be observed that Ga-MFI exhibits a CO_2 desorption peak at 139 °C, while Cu/Ga-MFI shows a significant shift in desorption temperature towards higher temperatures (180 °C and 289 °C), with a much wider CO_2 desorption peak compared that for Ga-MFI. CO_2-TPD results indicate that the introduction of Cu into Ga-MFI can effectively

enhance CO_2 adsorption capacity of the catalyst [47,48]. Considering that the products for CO_2-PDA reaction are complex and not easily distinguished through the in situ DRIFTs, the CO_2 activation process was simulated under a reductive atmosphere (H_2). Fig. 7b and c present the spectra of CO_2 hydrogenation over Cu/Ga-MFI and Ga-MFI at 550 °C, respectively. It can be found that, Cu/Ga-MFI exhibits distinct characteristic peaks of CO in 2000–2200 cm^{-1} [49–52], whereas Ga-MFI only exhibits a very weak peak in 2040–2060 cm^{-1}. This indicates that the introduction of Cu can effectively promote the activation of CO_2 under a reductive atmosphere through the RWGS, which thereby facilitate the removal of H during the CO_2-PDA reaction, favorably shifting the reaction equilibrium towards aromatics production [36]. Consequently, during the reaction process, Cu/Ga-MFI demonstrates higher propane and CO_2 conversion, as well as improved aromatics selectivity.

The CO_2-TPD and in situ DRIFTs results strongly demonstrate that the introduction of Cu into Ga-MFI can promote the adsorption and activation of CO_2, thereby assisting in propane dehydrogenation during CO_2-PDA reaction and enhancing the catalytic activity and aromatic selectivity of Cu/Ga-MFI.

3.5. Discussion on effects of CO_2

To investigate the influence of CO_2 during the process of propane aromatization (PDA), we compared the performance of Ga-MFI and Cu/Ga-MFI with and without of CO_2 in the feedstocks. As shown in Fig. 8, compared to the reaction in absence of CO_2, the propane conversion on both Ga-MFI and Cu/Ga-MFI were enhanced when CO_2 was passed through the reactor. Meanwhile, outstanding stability of the reaction can be observed on during the 600 min on stream. This can further confirm that CO_2 could promptly remove the reactive H species generated after propane dehydrogenation and promote the forward reaction of propane dehydrogenation, which is consisting with the literature [12, 36]. For Cu/Ga-MFI, the propane conversion decreased faster in the absence of CO_2. which means that CO_2 will help to inhibit the formation of coke on Cu/Ga-MFI during the CO_2-PDA reaction, thereby improving its catalytic stability. As a result, combined with the promote effect of Cu and CO_2, the Cu/Ga-MFI showed high activity, aromatic selectivity, and good stability.

Based on the above discussion, a possible reaction process for CO_2-PDA on Cu/Ga-MFI can be proposed as shown in Fig. 9. Specifically, C_3H_8 can be dehydrogenated on L acid sites to form C_3H_7 * and

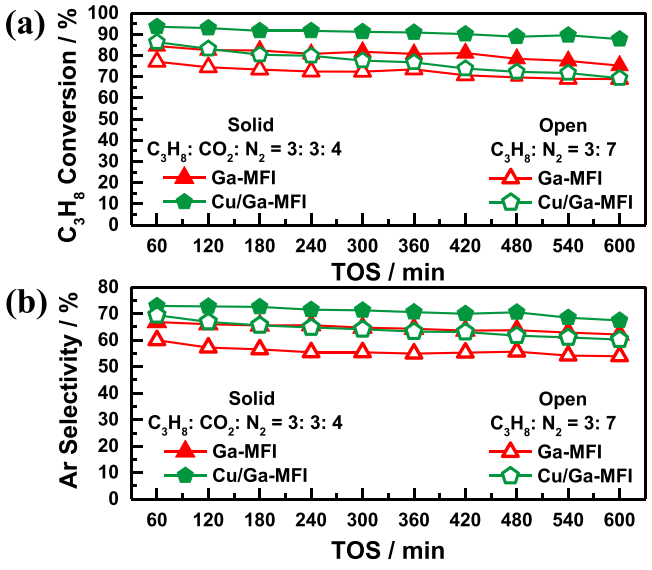

Fig. 8. (a) C_3H_8 conversion; and (b) aromatics selectivity of Ga-MFI and Cu/Ga-MFI under different reaction atmospheres. Reaction conditions: 0.3 g Catalysts (40–60 mesh); 1 atm; 600 °C, WHSV = 2000 mL·g^{-1}·h^{-1}.

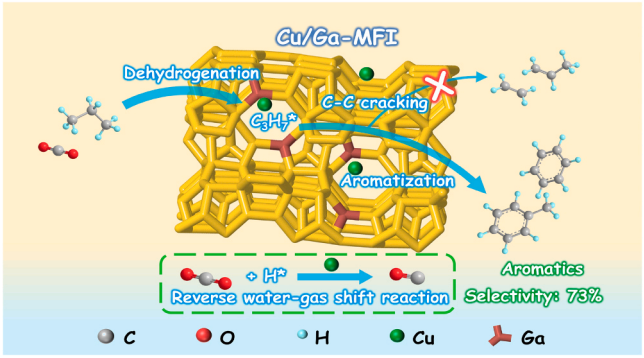

Fig. 9. The possible reaction process during CO_2-PDA for Cu/Ga-MFI.

H* species, and H* can be consumed with CO_2 with the help of Cu via a reverse water gas shift reaction. Subsequently, The C_3H_7 * continues to dehydrogenated to produce olefins, which undergo carbon-chain growth at the B-acid site and then dehydrogenated under the synergistic effect of L-acids adjacent to the B-acid to produce aromatics.

3.6. Stability, coke and regeneration

The generation of graphitic/polyaromatic carbon (coke) during the propane aromatization process is closely associated with excessive dehydrogenation of intermediates or over-polymerization of aromatics, resulting in carbon deposition and catalyst deactivation. The stability of each catalyst was evaluated (Fig. S12). Z5 exhibited good stability but poor aromatics selectivity. After the introduction of Ga or CuGa, Ga/Z5 and CuGa/Z5 showed significantly improved aromatic selectivity, while the propane conversion decreased rapidly from 90.9% to 55.8% and 87.2–27.1%, respectively, within the 1140 min of the reaction. Compared to Ga/Z5, CuGa/Z5 exhibited further enhanced aromatic selectivity. Cu modification of the Ga supported Z5 can enhance the aromatics selectivity and the initial activity, but it comes with a significant decrease in stability. This indicates a trade-off effect between aromatics selectivity and stability due to the presence of Al in the MFI framework and Cu modification for CuGa/Z5. In contrast, for Ga-MFI, due to the uniform distribution in the framework, Cu modification enables the formation of a proper B-L acid site pair involving Cu and the Ga-related B acid on the zeolite (Fig. S7b), which can not only assist in improving the dehydroaromatization of propane but also maintains high stability. Therefore, a high propane conversion above 67.5% with an average selectivity of 56.5% to aromatics can be achieved on Cu/Ga-MFI catalyst during the 1200 min reaction. Moreover, this could be attributed to the differences in coke deposition between CuGa/Z5 and Cu/Ga-MFI.

Toward this end, TG analysis was performed on the catalysts after the 1200 min reaction to investigate the coke deposition during the reaction process (Fig. 10a and Fig. S13a). As mentioned above, in the propane aromatization reaction, the conversion of propane and the selectivity towards aromatics have a significant interrelation with coke deposition on the catalyst. From Fig. 10a, it can be observed that Z5 has the lowest coke deposition (2.6%), while it exhibited the poorest aromatic selectivity but better stability. Combined with the DFT results, which might be due to the high activity in propane cracking, resulting in the production of methane and ethylene with less carbon deposition. Under similar aromatics selectivity, Cu/Ga-MFI demonstrated the best resistance to coke deposition, with a total coke deposition of approximately 6.0% after 1200 min. Furthermore, the TG results indicate that introducing CO_2 into the feedstocks can enhance the resistance of coke deposition for catalysts (Fig. S13a). This may be due to when presence of CO_2 can facilitate the removal of coke during the reaction through the Boudouard reaction ($CO_2 + C \rightarrow 2CO$), thereby improving the stability [10,36].

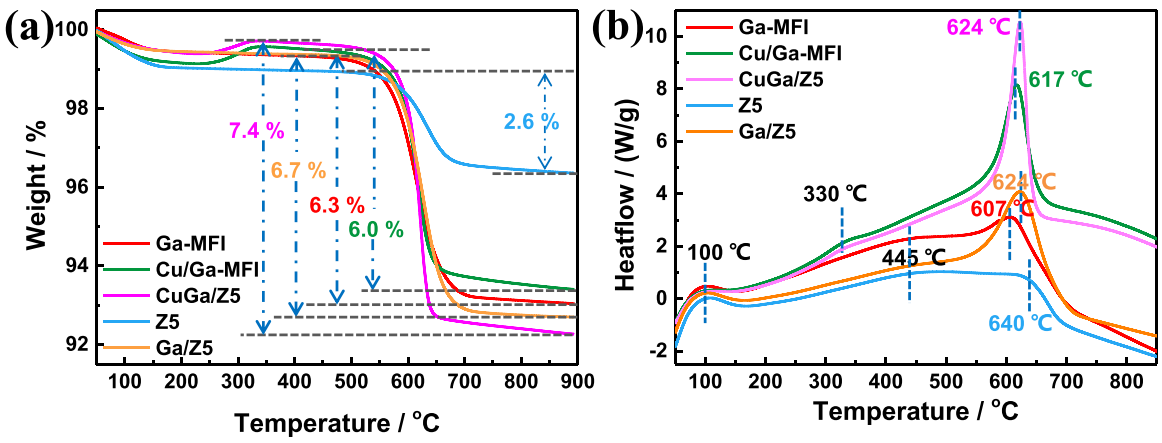

Fig. 10. (a) TG; and (b) DSC profiles of the spent catalysts after 1200 min CO_2-PDA reaction.

DSC analysis was simultaneously performed to assess the type and thermal stability of coke deposits formed during the PDA reaction. Generally, a higher temperature range of heat flow peaks in DSC indicates a higher stability of the coke, which require higher temperature for elimination by oxidants (i.e., CO_2 or O_2) [53]. In Fig. 10b, the peak around 100 °C corresponds to the water removal in the catalyst, while the peak near 330 °C may correspond to the oxidation of metallic Cu, and temperatures above 445 °C correspond to the oxidation of coke deposits in the catalyst. Compared to Z5 with Al in MFI framework, Ga-MFI exhibits a shift of the high-temperature peak towards lower temperatures (607 °C vs 640 °C), indicating that the Ga in the MFI framework not only effectively enhances aromatic selectivity but also suppresses carbon deposition and reduces the graphitization degree of the deposited carbon. This will be beneficial to catalyst regeneration at lower temperatures. With the introduction of Cu, Cu/Ga-MFI shows a slight shift of the high-temperature peak (617 °C) towards higher temperatures compared to that of Ga-MFI, and the disappearance of carbonaceous species around 445 °C. This may be attributed to the promotion of low-graphitized carbon precursors to convert into aromatics with the presence of Cu, leading to a higher proportion of highly graphitized carbon in the coke. Ga/Z5 and CuGa/Z5 exhibit the same peak temperature in the high-temperature region, both at 624 °C, indicating that the introduction of Cu has barely effect on the type of carbon deposition in Ga/Z5. Furthermore, the presence or absence of CO_2 does not affect the type of coke deposition on the catalyst (Fig. S13b).

The regeneration of Cu/Ga-MFI was conducted to investigate the relationship between catalyst deactivation and coke deposition. As shown in Fig. S14, after calcination for 6 h at 600 °C in air to remove the coke on the catalyst, the activity and aromatic selectivity of the Cu/Ga-MFI were completely restored and even slightly higher. This indicates that catalysts deactivation is primarily associated with carbon deposition. The improvement of catalytic performance after regeneration may be attributed to the enhanced dispersion of active metals in Cu/Ga-MFI during the regeneration process.

4. Conclusions

The Ga-MFI zeolite with framework Ga species was synthesized directly via a one-step hydrothermal method and employed in the CO_2-assisted propane dehydrogenation to aromatics. Compared to Al-MFI (Z5), Ga-MFI exhibited higher reaction activity and aromatics selectivity. Furthermore, Ga-MFI with framework Ga species showed superior reaction stability compared to Ga/Z5. NH_3-TPD, Py-IR, ICP-AES and DFT results indicated that the appropriate acidity of the B acid sites formed by Ga located in MFI framework, as well as the uniformly dispersion and coordination stability of Ga species within the zeolite, contributed to the enhanced dehydrogenation ability of Ga-MFI. The introduction of a second metal (Fe, Co, Cu, Zn or Pt) in Ga-MFI had a significant impact on the catalytic performance. Among them, Cu-modified Ga-MFI (Cu/Ga-MFI) exhibited the optimal activity and aromatics selectivity with good stability. CO_2-TPD and in situ DRIFTs results demonstrated that the introduction of Cu facilitated the adsorption and activation of CO_2, thereby promoting the removal of hydrogen through RWGS reaction during propane dehydrogenation and enhancing the reaction activity and aromatic selectivity. TG results revealed that the enhanced CO_2 activity also facilitated the removal of coke precursors, mitigating catalyst deactivation caused by coke deposition and prolonging the catalyst's lifetime. The Cu/Ga-MFI exhibits excellent cyclic regenerability and stability, maintaining high initial activity and aromatics selectivity even after 80 h of CO_2-PDA reaction. This study identified the optimal second metal additive and provided a foundation for the design of Ga-based MFI zeolite catalysts with uniformly dispersion and coordination stability Ga for high stability and aromatics selectivity CO_2-PDA reaction.

CRediT authorship contribution statement

Kankan Bu: Conceptualization, Investigation, Methodology, Writing – original draft. **Yikun Kang:** DFT calculations. **Yefei Li:** Resources, Writing-review & revision. **Yahong zhang:** Resources, Funding acquisition. **Yi Tang:** Resources, Funding acquisition. **Zhen Huang:** Formal analysis, Funding acquisition, Writing - review & revision. **Wei Shen:** Resources, Supervision, Funding acquisition, Writing-review & revision. **Hualong Xu:** Resources, Conceptualization, Supervision, Writing-review & revision, Funding acquisition.

Declaration of Competing Interest

The authors declare that they have no known competing financial interests or personal relationships that could have appeared to influence the work reported in this paper.

Data Availability

Data will be made available on request.

Acknowledgements

This work was financially supported by National Natural Science Foundation of China (22279021), National Key R&D Program of China (2018YFA0209402) and Shanghai Science and Technology Committee (Grant 14DZ2273900).

Appendix A. Supporting information

Supplementary data associated with this article can be found in the online version at doi:10.1016/j.apcatb.2023.123528.

References

[1] X. Guo, G. Fang, G. Li, H. Ma, H. Fan, L. Yu, C. Ma, X. Wu, D. Deng, M. Wei, D. Tan, R. Si, S. Zhang, J. Li, L. Sun, Z. Tang, X. Pan, X. Bao, Direct, nonoxidative conversion of methane to ethylene, aromatics, and hydrogen, Science 344 (2014) 616.

[2] N. Al-Yassir, M.N. Akhtar, S. Al-Khattaf, Physicochemical properties and catalytic performance of galloaluminosilicate in aromatization of lower alkanes: a comparative study with Ga/HZSM-5, J. Porous Mat. 19 (2012) 943–960.

[3] V.D. Rodrigues, F.J. Vasconcellos, A.D. Faro, Mechanistic studies through H-D exchange reactions: Propane aromatization in HZSM5 and Ga/HZSM5 catalysts, J. Catal. 344 (2016) 252–262.

[4] M. Migliori, A. Aloise, E. Catizzone, A. Caravella, G. Giordano, Simplified kinetic modeling of propane aromatization over Ga-ZSM-5 zeolites: comparison with experimental data, Ind. Eng. Chem. Res. 56 (2017) 10309–10317.

[5] A. Bhan, W.N. Delgass, Propane aromatization over HZSM-5 and Ga/HZSM-5 catalysts, Catal. Rev. Sci. Eng. 50 (2008) 19–151.

[6] S.W. Choi, W.G. Kim, J.S. So, J.S. Moore, Y. Liu, R.S. Dixit, J.G. Pendergast, C. Sievers, D.S. Sholl, S. Nair, C.W. Jones, Propane dehydrogenation catalyzed by gallosilicate MFI zeolites with perturbed acidity, J. Catal. 345 (2017) 113–123.

[7] E. Nowicka, C. Reece, S.M. Althahban, K.M.H. Mohammed, S.A. Kondrat, D. J. Morgan, Q. He, D.J. Willock, S. Golunski, C.J. Kiely, G.J. Hutchings, Elucidating the role of CO_2 in the soft oxidative dehydrogenation of propane over ceria-based catalysts, ACS Catal. 8 (2018) 3454–3468.

[8] F. Xing, J. Ma, K. i Shimizu, S. Furukawa, High-entropy intermetallics on ceria as efficient catalysts for the oxidative dehydrogenation of propane using CO_2, Nat. Commun. 13 (2022) 5065.

[9] T. Otroshchenko, G. Jiang, V.A. Kondratenko, U. Rodemerck, E.V. Kondratenko, Current status and perspectives in oxidative, non-oxidative and CO_2-mediated dehydrogenation of propane and isobutane over metal oxide catalysts, Chem. Soc. Rev. 50 (2021) 473–527.

[10] C. Tu, H. Fan, D. Wang, N. Rui, Y. Du, S.D. Senanayake, Z. Xie, X. Nie, J.G. Chen, CO_2-assisted ethane aromatization over zinc and phosphorous modified ZSM-5 catalysts, Appl. Catal. B Environ. 304 (2022).

[11] S. Yamauchi, A. Satsuma, S. Komai, T. Asakawa, T. Hattori, Y. Murakami, Zn-Loaded HZSM-5 for catalytic reduction of carbon dioxide by propane, in: J. Weitkamp, H.G. Karge, H. Pfeifer, W. Hölderich (Eds.), Stud. Surf. Sci. Catal., Elsevier, 1994, pp. 1571–1578.

[12] X. Niu, X. Nie, C. Yang, J.G. Chen, CO_2-Assisted propane aromatization over phosphorus-modified Ga/ZSM-5 catalysts, Catal. Sci. Technol. 10 (2020) 1881–1888.

[13] H. Xiao, J. Zhang, X. Wang, Q. Zhang, H. Xie, Y. Han, Y. Tan, A highly efficient Ga/ZSM-5 catalyst prepared by formic acid impregnation and in situ treatment for propane aromatization, Catal. Sci. Technol. 5 (2015) 4081–4090.

[14] G. Chen, L. Fang, T. Li, Y. Xiang, Ultralow-loading pt/zn hybrid cluster in zeolite hzsm-5 for efficient dehydroaromatization, J. Am. Chem. Soc. (2022).

[15] Vd.O. Rodrigues, J.G. Eon, A.C. Faro Jr., Correlations between dispersion, acidity, reducibility, and propane aromatization activity of gallium species supported on HZSM5 Zeolites, J. Phys. Chem. C. 114 (2010) 4557–4567.

[16] K. Sharifi, R. Halladj, S.J. Royaee, An overview on the effects of metal promoters and acidity of ZSM-5 in performance of the aromatization of liquid hydrocarbons, Rev. Adv. Mater. Sci. 59 (2020) 188–206.

[17] B.S. Kwak, W.M.H. Sachtler, Characterization and Testing of Ga/HZSM-5 Prepared by Sublimation of $GaCl_3$ into HZSM-5, J. Catal. 141 (1993) 729–732.

[18] I. Nowak, J. Quartararo, E.G. Derouane, J.C. Védrine, Effect of H_2–O_2 pre-treatments on the state of gallium in Ga/H-ZSM-5 propane aromatisation catalysts, Appl. Catal. A: Gen. 251 (2003) 107–120.

[19] V.R. Choudhary, A.K. Kinage, C. Sivadinarayana, M. Guisnet, Pulse reaction studies on variations of initial activity selectivity of O_2 and H_2 pretreated Ga-modified ZSM-5 type zeolite catalysts in propane aromatization, J. Catal. 158 (1996) 23–33.

[20] Y.H. Lim, M.Y. Gim, H. Kim, D.H. Kim, Top-down HCl treatment to prepare highly active Ga species in Ga/ZSM-5 for propane aromatization, Fuel Process. Technol. 227 (2022), 107107.

[21] M. Raad, A. Astafan, S. Hamieh, J. Toufaily, T. Hamieh, J.D. Comparot, C. Canaff, T.J. Daou, J. Patarin, L. Pinard, Catalytic properties of Ga-containing MFI-type zeolite in cyclohexane dehydrogenation and propane aromatization, J. Catal. 365 (2018) 376–390.

[22] A. Montes, G. Giannetto, A new way to obtain acid or bifunctional catalysts: V. Considerations on bifunctionality of the propane aromatization reaction over [Ga, Al]-ZSM-5 catalysts, Appl. Catal. A: Gen. 197 (2000) 31–39.

[23] K. Nishi, S. i Komai, K. Inagaki, A. Satsuma, T. Hattori, Structure and catalytic properties of Ga-MFI in propane aromatization, Appl. Catal. A: Gen. 223 (2002) 187–193.

[24] J. Kanai, N. Kawata, Aromatization of n-hexane over galloaluminosilicate and gallosilicate, Appl. Catal. 55 (1989) 115–122.

[25] N. Al-Yassir, M.N. Akhtar, K. Ogunronbi, S. Al-Khattaf, Synthesis of stable H-galloaluminosilicate MFI with hierarchical pore architecture by surfactant-mediated base hydrolysis, and their application in propane aromatization, J. Mol. Catal. A: Chem. 360 (2012) 1–15.

[26] C.R. Bayense, J.H.C. van Hooff, Aromatization of propane over gallium-containing H-ZSM-5 zeolites: Influence of the preparation method on the product selectivity and the catalytic stability, Appl. Catal. A: Gen. 79 (1991) 127–140.

[27] T. Inui, Y. Makino, F. Okazumi, A. Miyamoto, Selective conversion of propane into aromatics on platinum ion-exchanged gallium-silicate bifunctional catalysts, J. Chem. Soc., Chem. Commun. (1986) 571–573.

[28] U.V. Mentzel, K.T. Hojholt, M.S. Holm, R. Fehrmann, P. Beato, Conversion of methanol to hydrocarbons over conventional and mesoporous H-ZSM-5 and H-Ga-MFI: Major differences in deactivation behavior, Appl. Catal. A: Gen. 417 (2012) 290–297.

[29] R. Fricke, H. Kosslick, G. Lischke, M. Richter, Incorporation of Gallium into Zeolites: Syntheses, Properties and Catalytic Application, Chem. Rev. 100 (2000) 2303–2406.

[30] I. Yarulina, K. De Wispelaere, S. Bailleul, J. Goetze, M. Radersma, E. Abou-Hamad, I. Vollmer, M. Goesten, B. Mezari, E.J.M. Hensen, J.S. Martinez-Espin, M. Morten, S. Mitchell, J. Perez-Ramirez, U. Olsbye, B.M. Weckhuysen, V. Van Speybroeck, F. Kapteijn, J. Gascon, Structure-performance descriptors and the role of Lewis acidity in the methanol-to-propylene process, Nat. Chem. 10 (2018) 804–812.

[31] W. Zhou, J. Liu, L. Lin, X. Zhang, N. He, C. Liu, H. Guo, Enhanced dehydrogenative aromatization of propane by incorporating Fe and Pt into the Zn/HZSM-5 Catalyst, Ind. Eng. Chem. Res. 57 (2018) 16246–16256.

[32] L. Deng, J. Wang, Z. Wu, C. Liu, L. Qing, X. Liu, J. Xu, Z. Zhou, M. Xu, Effects of second metals (M = Fe, Cu, Ga, In, Sn) on the geometric and electronic properties of platinum for the direct dehydrogenation of propane, J. Alloy. Compd. 909 (2022), 164820.

[33] Y. Nakaya, F. Xing, H. Ham, K. i Shimizu, S. Furukawa, Doubly decorated platinum–gallium intermetallics as stable catalysts for propane dehydrogenation, Angew. Chem. Int. Ed. 60 (2021) 19715–19719.

[34] G.G. Oseke, A.Y. Atta, B. Mukhtar, B.J. El-Yakubu, B.O. Aderemi, Increasing the catalytic stability of microporous Zn/ZSM-5 with copper for enhanced propane aromatization, J. King Saud. Univ., Eng. Sci. 33 (2021) 531–538.

[35] D. Liu, L. Cao, G. Zhang, L. Zhao, J. Gao, C. Xu, Catalytic conversion of light alkanes to aromatics by metal-containing HZSM-5 zeolite catalysts—a review, Fuel Process. Technol. 216 (2021), 106770.

[36] H. Fan, X. Nie, C. Song, X. Guo, Mechanistic insight into the promotional effect of CO_2 on propane aromatization over Zn/ZSM-5, Ind. Eng. Chem. Res. 61 (2022) 10483–10495.

[37] Z. Han, F. Zhou, Y. Liu, K. Qiao, H. Ma, L. Yu, G. Wu, Synthesis of gallium-containing ZSM-5 zeolites by the seed-induced method and catalytic performance of GaZSM-5 and AlZSM-5 during the conversion of methanol to olefins, J. Taiwan Inst. Chem. Eng. 103 (2019) 149–159.

[38] B. Puértolas, L. García-Andújar, T. García, M.V. Navarro, S. Mitchell, J. Pérez-Ramírez, Bifunctional Cu/H-ZSM-5 zeolite with hierarchical porosity for hydrocarbon abatement under cold-start conditions, Appl. Catal. B Environ. 154–155 (2014) 161–170.

[39] M.W. Schreiber, C.P. Plaisance, M. Baumgärtl, K. Reuter, A. Jentys, R. Bermejo-Deval, J.A. Lercher, Lewis-brønsted acid pairs in Ga/H-ZSM-5 to catalyze dehydrogenation of light alkanes, J. Am. Chem. Soc. 140 (2018) 4849–4859.

[40] S. Wang, Z. Huang, Y.J. Luo, J.H. Wang, Y. Fang, W.M. Hua, Y.H. Yue, H.L. Xu, W. Shen, Direct conversion of syngas into light aromatics over Cu-promoted ZSM-5 with ceria-zirconia solid solution, Catal. Sci. Technol. 10 (2020) 6562–6572.

[41] M.Y. Gim, C. Song, Y.H. Lim, K.Y. Lee, D.H. Kim, Effect of the Si/Al ratio in Ga/mesoporous HZSM-5 on the production of benzene, toluene, and xylene via coaromatization of methane and propane, Catal. Sci. Technol. 9 (2019) 6285–6296.

[42] A.M. Hengne, K.D. Bhatte, S. Ould-Chikh, Y. Saih, J.M. Basset, K.W. Huang, Selective production of oxygenates from carbon dioxide hydrogenation over a mesoporous-silica-supported copper-gallium nanocomposite catalyst, ChemCatChem 10 (2018) 1360–1369.

[43] L. Wang, W. Li, G. Qi, D. Weng, Location and nature of Cu species in Cu/SAPO-34 for selective catalytic reduction of NO with NH3, J. Catal. 289 (2012) 21–29.

[44] D. Nozik, A.T. Bell, Role of Ga^{3+} sites in ethene oligomerization over Ga/H-MFI, ACS Catal. 12 (2022) 14173–14184.

[45] P. Gao, Q. Wang, J. Xu, G. Qi, C. Wang, X. Zhou, X. Zhao, N. Feng, X. Liu, F. Deng, Brønsted/Lewis acid synergy in methanol-to-aromatics conversion on ga-modified zsm-5 zeolites, as studied by solid-state NMR spectroscopy, ACS Catal. 8 (2018) 69–74.

[46] H. Xiao, J. Zhang, P. Wang, Z. Zhang, Q. Zhang, H. Xie, G. Yang, Y. Han, Y. Tan, Mechanistic insight to acidity effects of Ga/HZSM-5 on its activity for propane aromatization, RSC Adv. 5 (2015) 92222–92233.

[47] H. Tian, J. Jiao, F. Zha, X. Guo, X. Tang, Y. Chang, H. Chen, Hydrogenation of CO_2 into aromatics over ZnZrO-Zn/HZSM-5 composite catalysts derived from ZIF-8, Catal. Sci. Technol. 12 (2022) 799–811.

[48] S. Chen, J. Zhang, F. Song, Q. Zhang, G. Yang, M. Zhang, X. Wang, H. Xie, Y. Tan, Induced high selectivity methanol formation during CO_2 hydrogenation over a $CuBr_2$-modified CuZnZr catalyst, J. Catal. 389 (2020) 47–59.

[49] X. Yang, Y. Wei, Y. Su, L. Zhou, Characterization of fused Fe-Cu based catalyst for higher alcohols synthesis and DRIFTS investigation of TPSR, Fuel Process. Technol. 91 (2010) 1168–1173.

[50] C. Dossi, S. Recchia, A. Pozzi, A. Fusi, V. Dalsanto, G. Moretti, In situ analytical investigation of redox behavior of Cu-ZSM-5 catalysts, Phys. Chem. Chem. Phys. 1 (1999) 4515–4519.

[51] C. Márquez-Alvarez, G.S. McDougall, A. Guerrero-Ruiz, I. Rodríguez-Ramos, Study of the surface species formed from the interaction of NO and CO with copper ions in ZSM-5 and Y zeolites, Appl. Surf. Sci. 78 (1994) 477–484.
[52] M. Bersani, K. Gupta, A.K. Mishra, R. Lanza, S.F.R. Taylor, H.U. Islam, N. Hollingsworth, C. Hardacre, N.H. de Leeuw, J.A. Darr, Combined EXAFS, XRD, DRIFTS, and DFT Study of Nano Copper-Based Catalysts for CO_2 Hydrogenation, ACS Catal. 6 (2016) 5823–5833.
[53] W. Hally, J.H. Bitter, K. Seshan, J.A. Lercher, J.R.H. Ross, Problem of coke formation on Ni/ZrO_2 catalysts during the carbon dioxide reforming of methane, in: B. Delmon, G.F. Froment (Eds.), Stud. Surf. Sci. Catal., Elsevier, 1994, pp. 167–173.